Microfluid Nanofluid (2008) 5:215–224
DOI 10.1007/s10404-007-0239-3

RESEARCH PAPER

Aerosol flow through a long micro-capillary: collimated aerosol beam

I. S. Akhatov · J. M. Hoey · O. F. Swenson · D. L. Schulz

Received: 12 September 2007 / Accepted: 30 October 2007 / Published online: 14 November 2007

Abstract A micro-capillary system capable of generating a focused collimated aerosol beam (CAB) is demonstrated both theoretically and experimentally. The approach is based on a manifestation of the Saffman force where high velocity (~100 m/s) aerosol particles, flowing through a micro-capillary ($d \sim 100$ μm and $l \sim 1$ cm), migrate perpendicular to the centerline of the capillary. Upon exiting the micro-capillary system, the particles maintain momentum, and when the aerosol is comprised of solid-in-liquid dispersions such as Ag nanoparticle ink, the CAB approach enables printing of advanced materials features with linewidth ≤ 10 μm.

Keywords Aerosol · Focusing · Beam collimation · Micro-capillary · Saffman force · Direct-write fabrication

1 Introduction

Gas flow through small channels has become an intriguing research topic that has led to the emergence of a new branch of fluid dynamics—"microfluidics". It is well established that the violation of the "no-slip boundary condition" for a fluid near a solid wall is a key microfluidics phenomenon (see Karniadakis et al. 2005; Lauga et al. 2005, for exhaustive reviews). In this paper we discuss micron size aerosol micro-flow through a capillary of radius ~100 μm and length ~1 cm. The no-slip boundary condition at the capillary wall is valid in this case since the capillary radius is much larger than the mean free path of the gas molecules (~100 nm). However, at a relatively high velocity of ~100 m/s, such an aerosol flow reveals a new manifestation of microfluidics: the Saffman force acting on aerosol particles in gas flowing through a micro-capillary becomes significant thereby causing noticeable migration of particles toward the center line of the capillary (Akhatov et al. 2007). The logical extension of these results are reported in the present paper where we have the following two aims: firstly, the design of a micro-capillary ("aerosol gun") capable of generating a focused collimated aerosol beam (CAB) in which aerosol particles stay very close to a capillary center line is shown feasible theoretically and experimentally; and secondly, the performance of such an aerosol gun for printing solid features on a substrate is demonstrated.

The paper begins with a review of the aerodynamic focusing concept, experimental and theoretical evaluations of the significance of the Saffman force in aerosol flows. Also included in the Sect. 1 is a description of how these flows are applied in direct-write fabrication (i.e., printing an ink) technology. In Sect. 2, the mathematical model for aerosol flow in a micro-capillary that we previously detailed and verified experimentally (Akhatov et al. 2007) is presented in brief. The concept of a focused collimated aerosol beam for direct-write fabrication is presented in Sect. 3 and the development of a method of generating a CAB using a micro-capillary of slowly varying radius is discussed. Here we also design a new micro-capillary

I. S. Akhatov (✉) · J. M. Hoey · D. L. Schulz
Department of Mechanical Engineering,
North Dakota State University, Fargo, ND 58105, USA
e-mail: Iskander.Akhatov@ndsu.edu

O. F. Swenson
Department of Physics, North Dakota State University,
Fargo, ND 58105, USA

I. S. Akhatov · J. M. Hoey · O. F. Swenson · D. L. Schulz
Center for Nanoscale Science and Engineering,
North Dakota State University, Fargo, ND 58105, USA

direct-write system (CAB-DW) that can be used to generate and deposit a focused collimated aerosol beam. Finally, the CAB-DW system is tested experimentally in Sect. 4 where a reasonable match between theoretical predictions and experimental observations of CAB-DW is demonstrated.

1.1 Aerodynamic focusing concept

When an aerosol flows through a converging nozzle, the particles may focus downstream from the nozzle (Israel and Friedlander 1967; Dahneke and Friedlander 1970; Israel and Wang 1971). Israel and Friedlander (1967) first showed that aerosol focusing is a consequence of inertial effects where the particles obtain a radially inward motion during acceleration through a converging nozzle. This radial motion is retained downstream of the nozzle even as the rapidly expanding carrier gas diverges radially outward. Fernandez de la Mora and Riesco-Chueca (1988) showed that the particles originating upstream near the symmetry axis may cross it at a common focal point downstream from the nozzle exit. In that theoretical study, the motion of aerosol particles suspended in a carrier gas was described in terms of particle inertia and Stokes drag using Newton's equation of motion. These experimental and theoretical findings served as a background for subsequent extensive experimental and numerical studies of aerodynamic focusing of aerosol particles (Rao et al. 1993; Fuerstenau et al. 1994; and references therein).

The aforementioned classic aerodynamic focusing concept normally deals with thin plate orifices or abruptly converging nozzles. The present paper examines the case of a relatively long nozzle that might be better termed a micro-capillary with a radius of $\sim$100 μm, length of $\sim$1 cm and a slowly varying inner diameter. The underlying premise of our approach is that the Saffman force acts on aerosol particles in gas flowing through a micro-capillary thereby causing noticeable migration of particles perpendicular to the centerline of the tube. This novel idea is in contrast to the classical aerodynamic focusing method where only particle inertia and Stokes drag force are used to characterize gas-particle interactions.

1.2 The Saffman force in aerosol flows

Interest in the motion of small particles carried along by fluid flow through straight tubes has been stimulated in the past by observations of Poiseuille that red blood cells tend to avoid vessel walls when flowing through capillaries. This observation sparked research interest in particle migration in shear flows. At that time, it was understood that small particles in a shear flow experience a force perpendicular to the direction of flow. An expression for this force was first obtained by Saffman (1965, 1968) for a small sphere in an unbounded shear flow. It was shown that the direction of this Saffman force depends on the product $(u - u_p)(\partial u/\partial y)$, where u and u_p are the velocities of the fluid and the particle respectively in the x direction. If the particle is being dragged by the fluid ($u - u_p > 0$) as shown on Fig. 1, the resultant force pushes the particle to the region where the fluid velocity is higher. Conversely, if the particle is dragging the fluid ($u - u_p < 0$), the resultant force pushes the particle to the region where the fluid velocity is lower.

Two examples of indirect experimental and theoretical evaluations of the significance of the Saffman force in conventional (macroscale) aerosol flows have been reported. Firstly, since the particle density is higher than the gas density in an aerosol flow, single particles should migrate towards the duct walls in downflows (i.e., with the force of gravity) or toward the duct axis in upflows (i.e., against gravity). This effect was experimentally verified by Lipatov et al. (1989) where the efficiency of particle deposition on the inner walls of upright ducts in upflow and downflow conditions was determined. The satisfactory agreement of the experimental and theoretical results for downflows and the negligible inner particle deposition for upflows provided an indirect confirmation of the significance of the Saffman force in aerosol flows.

Secondly, it has been established experimentally that shock and detonation waves propagated along dusty surfaces may cause particles to be entrained away from the near-wall region (Fletcher 1976; Merzkirch and Bracht 1978). In this situation, several possible mechanisms of dust rise, which predominate under different flow conditions, were discussed (Gerrard 1963; Bracht and Merzkirch 1979; Hishida and Hayashi 1989). The importance of taking the Saffman force into account was noted by Merzkirch and Bracht (1978) and Hwang (1986) who calculated the

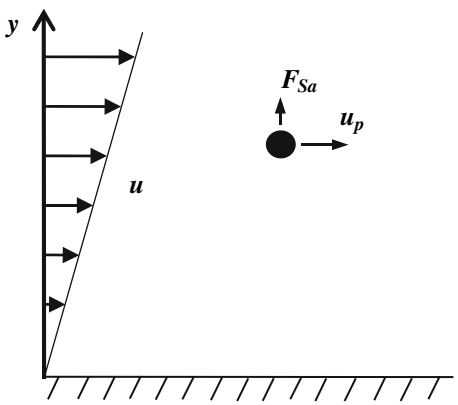

Fig. 1 Schematic of a particle dragged by a shear flow

trajectory of a single sphere initially located on a plane surface and set in motion by a shock wave propagating along this surface. High-speed cinematographic experiments performed with a shock tube allowed mapping of the dust cloud. From the agreement between the measured shape of the cloud and the calculated trajectories of the flight of the particles, it was concluded that a Saffman force-based model for the motion of the particles adequately describes the removal of particles from the wall.

A review of mathematical modeling that included the Saffman force effect on the formation of local particle accumulation zones in various shear flows was presented by Osiptsov (1997). In particular, Osiptsov (1988) studied the motion of particles at the entrance zones to a flat channel and a circular pipe.

The systematic theoretical and experimental study of the impact of the Saffman force on aerosol micro-flows was presented by Akhatov et al (2007) who developed a mathematical model that accounted for complicated interactions between aerosol particles and carrier gas flowing through a micro-capillary. It was experimentally verified by visualization (i.e., laser scattering imaged with an optical microscope) of an aerosol beam of particles (i.e., silver-ink particles $d \sim 0.5$ μm) exiting a micro-capillary. These experimentally verified theoretical predictions serve as the basis of a new concept for controlling and optimizing focused aerosol beams through long micro-capillaries.

1.3 Direct-write fabrication

The term direct-write encompasses film deposition processes whereby no additional processing steps (e.g., photolithography) are required to produce patterned functional structures of electronic materials such as metallic interconnects and semiconductor diodes and transistors. Direct-write includes conventional approaches such as airbrush spray deposition and ink-jet printing as well as more esoteric methods such as matrix-assisted pulsed laser evaporation direct-write (MAPLE-DW). Direct-write fabrication of electronic components represents a research area that has been active for years with special emphasis on technology development for fabrication of electronic and sensor devices (Pique and Chrisey 2002). One direct-write technology that utilizes a focused aerosol beam is termed Maskless Mesoscale Material Deposition (M^3D^{TM}) aerosol jet deposition system, developed by Renn et al. (2002) and now being commercialized by Optomec Inc. A schematic of the M^3D direct-write fabrication technique is presented in Fig. 2. According to this concept, an aerosol beam flows out of a relatively long, gradually converging micro-capillary. Being somewhat focused due to the converging

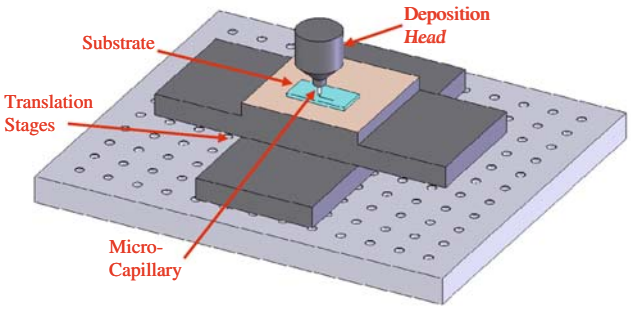

Fig. 2 Schematic of a direct-write fabrication technique that utilizes a focused aerosol beam

geometry of the micro-capillary, the aerosol beam hits a substrate resulting in materials deposition. This technology allows the deposition of 25 μm-wide lines but suffers from materials utilization and overspray limitations (Renn et al. 2002).

Process improvements realized in the present paper using the new theoretical model developed in Akhatov et al. (2007) will allow the CAB deposition of features ≤10 μm in width with minimal overspray. Upon appropriate development of the precursor inks, CAB-DW will be enabling for the manufacture of flexible microelectronics such as radio frequency identification (RFID), disposable wireless sensors and large-area displays/signs. The knowledge of how to manipulate aerosol beams in micro-scale has application not only in direct write fabrication but also in materials processing such as gas-phase formation of nanoparticles. The successful development of adequate theoretical models and numerical codes for aerosol dynamics at the micro-scale will have a significant impact on the progress of these technological processes.

2 The mathematical model for aerosol flow in a slowly varying micro-capillary

In this section we briefly present the mathematical model for aerosol flow in a micro-capillary discussed in detail and verified experimentally in Akhatov et al. (2007). Generally, there are the following forces of interaction between a particle and a carrier gas flow: (1) the Stokes drag force, which represents a steady viscous drag force; (2) the Basset force, which represents a non-steady viscous drag force; (3) virtual mass force, which represents the inertia of the fluid around a particle added to that particle; (4) fluid pressure gradient force; (5) gravity force; (6) the Magnus force, which represents a steady lift force of a viscous fluid on a rotating particle; (7) the Saffman force, which represents a steady lift force induced by the local shear flow of a viscous fluid. In this model we account only for the Stokes and

the Saffman forces, since the other forces are negligible for our applications.

The Stokes drag force is calculated as follows:

$$\begin{aligned}
&\mathbf{F}_{St} = 6\pi a\mu(\mathbf{v}-\mathbf{v}_\mathrm{p})\frac{C_{St}}{C_{Kn}},\\
&C_{St} = \left(1+\frac{1}{6}Re_\mathrm{p}^{2/3}\right)\left[1+\exp\left(-\frac{0.427}{Ma_\mathrm{p}^{4.63}}-\frac{3}{Re_\mathrm{p}^{0.88}}\right)\right],\\
&C_{Kn} = 1+Kn_\mathrm{p}\left[2.57+0.68\exp\left(-\frac{1.86}{Kn_\mathrm{p}}\right)\right],\\
&Re_\mathrm{p} = \frac{2a\rho|\mathbf{v}-\mathbf{v}_\mathrm{p}|}{\mu},\quad Ma_\mathrm{p} = \frac{|\mathbf{v}-\mathbf{v}_\mathrm{p}|}{c},\quad Kn_\mathrm{p} = \frac{l}{2a}
\end{aligned} \tag{1}$$

where c, l are the sound and mean free path in the fluid, $\mathbf{v}$, $\mathbf{v}_\mathrm{p}$ are the vector velocities of the fluid and particle, and C_{St}, C_{Kn} are correction factors that take into account the deviation of the particle drag from Stokes law $\mathbf{F}_{St} = 6\pi a\mu(\mathbf{v}-\mathbf{v}_\mathrm{p})$. The function C_{St} takes into account the deviation of the particle drag from Stokes law due to finite Reynolds number Re_p and Mach number Ma_p (Carlson and Hoglund 1964). The function C_Kn takes into account the deviation of the particle drag from Stokes law due to a finite Knudsen number, Kn_p, (Cunningham 1910; Knudsen and Weber 1911; Millikan 1923; Li and Wang 2003; Wang et al. 2005a, b, c).

An expression for the steady lift force induced by the local shear flow of a viscous fluid on a sphere was given by Saffman (1965, 1968). It was systematically derived that a spherical particle of radius a moving along the x-axis such that $\mathbf{v}_\mathrm{p} = (u_\mathrm{p}, 0, 0)$ in a fluid shear flow field $\mathbf{v}(u(y),0,0)$ experiences a force directed along the y-axis which can be calculated as follows:

$$\mathbf{F}_{Sa} = 6.46\, a^2(u-u_\mathrm{p})\sqrt{\rho\mu\left|\frac{\partial u}{\partial y}\right|}\,\mathrm{Sign}\left(\frac{\partial u}{\partial y}\right)\mathbf{e}_y \tag{2}$$

where $\mathbf{e}_y$ is a unit vector directed along the y-axis (Fig. 1). In the derivation by Saffman (1965, 1968) it was assumed that

$$Re_\mathrm{p} \ll 1,\quad Re_\mathrm{f} = \frac{a^2\rho}{\mu}\left|\frac{\partial u}{\partial y}\right| \ll 1,\quad Re_\mathrm{p} \ll Re_\mathrm{f}^{1/2} \tag{3}$$

Some corrections must be implemented in order to apply the Saffman force for a broader range of parameters. Then Eq. (2) becomes

$$\begin{aligned}
&\mathbf{F}_{Sa} = 6.46\, a^2(u-u_\mathrm{p})\sqrt{\rho\mu\left|\frac{\partial u}{\partial y}\right|}\,\mathrm{Sign}\left(\frac{\partial u}{\partial y}\right)C_{Sa}\,\mathbf{e}_y,\\
&C_{Sa} = \begin{cases}
0.23434\left[1-\exp\left(-0.1Re_\mathrm{p}\right)\right]\dfrac{Re_\mathrm{f}}{Re_\mathrm{p}} & \\
\quad +\exp\left(-0.1Re_\mathrm{p}\right), & Re_\mathrm{p} < 40\\
0.0371Re_\mathrm{f}^{1/2}, & Re_\mathrm{p} \geq 40
\end{cases}
\end{aligned} \tag{4}$$

The function C_{Sa} takes into account the deviation of the particle lift force from the Saffman law, Eq. (2), due to finite Reynolds numbers, Re_p (Dandy and Dwyer 1990; Mei 1992).

In our calculations the maximal values of Reynolds and Mach numbers of the gas flow around the particles were $Re_\mathrm{p} \sim 2$ and $Ma_\mathrm{p} \sim 0.1$. It was found, at that moment, that $Re_\mathrm{f} \sim 0.025$. Note that Knudsen number is not taken into account in the Saffman force.

We consider relatively fast aerosol flows through micro-capillaries. A simple estimation shows that for nitrogen gas flowing with a mean velocity of 50 m/s through a micro-capillary of diameter D = 100 μm, the Reynolds number is about Re = 350. So, the flow is laminar. The entrance length, L_e, needed for such a flow to become fully developed can be calculated from the equation $L_\mathrm{e}/D \approx 0.06Re$ (Batchelor 2000), that gives $L_\mathrm{e} \approx 0.2$ cm. Thus, such a flow can be treated as a steady laminar Pouseuille flow if the capillary length $L \gg L_\mathrm{e} \approx 0.2$ cm. In the parameter range that we consider in this study, gas compressibility essentially does not affect the aerosol flow; consequently, we use the incompressible gas approximation.

Let us also estimate the characteristic particle velocity relaxation length. The particle viscous relaxation time, τ_μ, after which the particle velocity is almost equal to the fluid velocity due to the Stokes drag force, can be calculated as $\tau_\mu = 2a^2\rho_\mathrm{p}/9\mu$. For example, if $a = 0.5$ μm, $\mu = 1.8 \times 10^{-5}$ kg/(m s) (nitrogen gas), ρ_p = 2,000 kg/m^3, one has $\tau_\mu \sim 6$ μs. During this time, being dragged by the flow of $\bar{u} = 50$ m/s, the aerosol particles will travel a distance of $L_\mu \sim \bar{u}\tau_\mu \sim 0.3$ mm. That means that for a relatively long capillary, $L \gg L_\mu$ there is a very small velocity difference between the particles and the gas.

Thus, we consider here aerosol particles moving in a steady laminar Pouseuille incompressible flow through a micro-capillary of slowly varying radius. To make it specific, and to prepare for a comparison with experiment that will be presented in the next section, we consider the case of a slowly converging or diverging micro-capillary, such that its radius changes linearly with its length

$$R(x) = R_1 - \frac{R_1-R_2}{L}x \tag{5}$$

Here R_1, R_2 are capillary radii at the beginning and at the end respectively.

To make calculations as simple as possible, we are assuming here a parabolic Pouseuille velocity distribution in every capillary cross-section. Indeed, if the radius of the micro-capillary slowly changes, the inertial effects in both the radial and the longitudinal directions can be neglected when (Batchelor 2000)

$$\left(\frac{R_1-R_2}{L}\right)\frac{\bar{u}D\rho}{\mu} \ll 1 \tag{6}$$

If the length of the micro-capillary is not large enough to satisfy the inequality (6) then there is some inherent error due to the inertial forces and a more advanced CFD modeling of the gas flow in such a micro-capillary may be needed.

The parabolic gas velocity distribution across the micro-capillary can be presented as follows

$$u = u_{\max}(x)\left(1 - \frac{r^2}{R^2(x)}\right), \quad u_{\max}(x) = \frac{2Q}{\pi R^2(x)} \tag{7}$$

where Q is the volumetric gas flowrate through the micro-capillary. The streamlines are not exactly unidirectional but are inclined to the axis at a small angle, as shown in Fig. 3. In addition to the axial component of velocity, u, presented in Eq. (7), there is a radial component, v, such that

$$\begin{aligned} &\mathbf{v} = u\mathbf{e}_x + v\mathbf{e}_r, \quad v = -\tan(\alpha)u, \\ &\tan(\alpha) = \left(1 - \frac{R_2}{R_1}\right)\frac{R_1}{L}\frac{r}{R(x)} \end{aligned} \tag{8}$$

Given the gas velocity distribution (7) and (8), we are going to calculate the particle trajectories in such a flow. The equation of motion of a single particle is

$$\frac{4}{3}\pi a^3 \rho_{\mathrm{p}} \frac{\mathrm{d}\mathbf{v}_{\mathrm{p}}}{\mathrm{d}t} = \mathbf{F}_{St} + \mathbf{F}_{Sa} \tag{9}$$

Here $\mathbf{F}_{St}$ and $\mathbf{F}_{Sa}$ are the Stokes and the Saffman forces presented in the Eqs. (1) and (4) respectively. Note that the variable y in Eq. (4) should be replaced by the variable r.

It is natural to introduce the following dimensionless variables

$$\begin{aligned} &\bar{t} = \frac{t}{\tau_\mu}, \quad \bar{x}_{\mathrm{p}} = \frac{x_{\mathrm{p}}}{L}, \quad \bar{r}_{\mathrm{p}} = \frac{r_{\mathrm{p}}}{R_1}, \quad \bar{u}_{\mathrm{p}} = \frac{u_{\mathrm{p}}}{u_*}, \quad \bar{u} = \frac{u}{u_*}, \\ &\bar{v}_{\mathrm{p}} = \frac{v_{\mathrm{p}}}{v_*}, \quad u_* = \frac{L}{\tau_\mu}, \quad v_* = \frac{R_1}{\tau_\mu}, \quad \tau_\mu = \frac{2a^2\rho_{\mathrm{p}}}{9\mu} \end{aligned} \tag{10}$$

Then the equations of particle motion (9) can be presented in a form

$$\begin{aligned} &\frac{\mathrm{d}\bar{x}_{\mathrm{p}}}{\mathrm{d}\bar{t}} = \bar{u}_{\mathrm{p}}, \quad \frac{\mathrm{d}\bar{r}_{\mathrm{p}}}{\mathrm{d}\bar{t}} = \bar{v}_{\mathrm{p}}, \\ &\frac{\mathrm{d}\bar{u}_{\mathrm{p}}}{\mathrm{d}\bar{t}} = \frac{C_{St}}{C_{Kn}}\left(\bar{u} - \bar{u}_{\mathrm{p}}\right), \\ &\frac{\mathrm{d}\bar{v}_{\mathrm{p}}}{\mathrm{d}\bar{t}} = \frac{C_{St}}{C_{Kn}}\left(\bar{v} - \bar{v}_{\mathrm{p}}\right) - \kappa C_{Sa}\left(\bar{u} - \bar{u}_{\mathrm{p}}\right)\frac{\sqrt{\bar{r}_{\mathrm{p}}}}{\bar{R}^2(\bar{x}_{\mathrm{p}})}, \\ &\bar{u} = \varepsilon S \frac{\bar{R}^2(\bar{x}_{\mathrm{p}}) - \bar{r}_{\mathrm{p}}^2}{\bar{R}^4(\bar{x}_{\mathrm{p}})}, \quad \bar{R}(\bar{x}_{\mathrm{p}}) = 1 - \frac{R_1 - R_2}{L}\bar{x}_{\mathrm{p}} \end{aligned} \tag{11}$$

Here C_{St}, C_{Kn}, C_{Sa} are the correction functions for the Stokes and Saffman forces presented in the Eqs. (1) and (4); ε is the geometrical parameter

$$\varepsilon = \frac{R_1}{L} \tag{12}$$

S is the Stokes number

$$S = \frac{\tau_\mu u_{\max}(0)}{R_1}, \quad u_{\max}(0) = \frac{2Q}{\pi R_1^2}, \tag{13}$$

and κ is the dimensionless parameter responsible for the contribution of the Saffman force on particle motion in an aerosol flow. It can be represented as a function of the Stokes number, S, and geometrical parameter, ε, as follows

$$\kappa = \frac{3.23}{\pi\varepsilon}\sqrt{\frac{S}{\delta}}, \quad \delta = \frac{\rho_{\mathrm{p}}}{\rho} \tag{14}$$

It is clear from such a dimensionless representation (11) that for a given Stokes number the contribution of the Saffman force is greater for smaller ε (longer capillaries).

Having this mathematical model, it is possible to calculate trajectories of aerosol particles in a slowly varying micro-capillary of any shape that is used in experiments. Aluminum oxide micro-capillaries from Gaiser Tool (Ventura, CA) were used in these experiments. The internal geometry was verified by imaging the micro-capillary using a Dage XD7600NT X-ray imaging system with the X-ray images from one of the capillaries shown in Fig. 4. In this picture it is clearly visible that the micro-capillary's

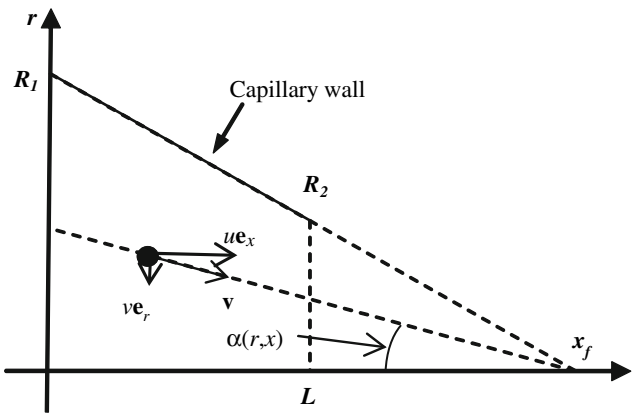

Fig. 3 Axial and radial gas velocity components in a slowly converging micro-capillary

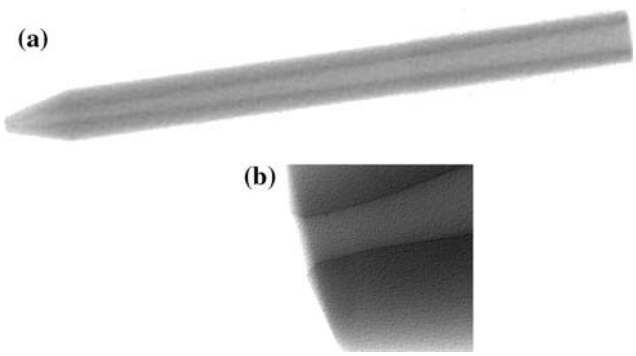

Fig. 4 X-ray imaging of one of the Gaiser Tool Inc. aluminum oxide micro-capillaries (100 μm diameter) used in the experiments

internal radius changes linearly with length (Fig. 4a); however, it is not perfectly linear at the immediate exit (Fig. 4b).

In Akhatov et al. (2007) we have presented results of calculations for such a micro-capillary with $R_1 = 400$ μm, $R_2 = 50$ μm, a nitrogen carrier gas flow of $Q = 40$ cm^3/min and aerosol particles with material density $\rho_p = 2{,}000$ kg/m^3, and of size $a = 0.5$ μm. We calculated the trajectories of particles with and without the Saffman force acting on them. Before entering the micro-capillary, particles move along with the gas flow through a relatively long tube. That is why in all of our calculations we set the entrance particle velocity equal to the gas velocity. Our calculations show, however, that in cases considered in this paper, particle trajectories do not depend on the magnitude of the particle's entrance velocity. It was also assumed that after the particles exit the capillary, they fly by inertia only. The calculations have shown that all the particles of this size migrate towards the centerline forming a focal spot immediately following the capillary exit. This migration is caused by both the geometrical convergence of the capillary and the Saffman force.

The geometrical convergence was clearly illustrated by calculating particle trajectories driven only by inertia and the Stokes drag (no Saffman force). In this case all of the particles came to a very fine geometrical focal spot denoted in Fig. 3 as x_f, which was about 3 mm apart from the capillary exit. The contribution of the Saffman force noticeably changed the position of the focal spot, which now comes closer to the capillary exit, about 1.5 mm apart from it. It was also noticed that the diameter of this focal point increased up to about 5 μm. These theoretical results were verified with experimental observations of an aerosol beam coming out of such a micro-capillary. It was shown that while the theoretical model that uses only the Stokes drag force does not correlate to the experimental data; the model that considers both Stokes and Saffman forces closely matches the experimental data.

3 The concept of a collimated aerosol beam

The difference between calculations with and without the Saffman force suggested that in order to design an effective aerosol focusing apparatus in this range of parameters, one must account for the Saffman force. Moreover, it suggested that the Saffman force is not necessarily playing a positive role in the aerosol focusing process from the stand point of direct-write fabrication technology. Indeed, for the case described in the previous section, the Saffman force has a deleterious effect on direct-write deposition as follows. Consider that one is using a micro-capillary to deposit small features on a substrate (see Fig. 2). Saffman forces cause the particle trajectories to focus closer to the capillary exit and diverge much faster after the focal point than they would in the case of simple geometrical focusing due to the Stokes drag force only. Consequently, precise control of the tip-to-substrate distance is required to assure the beam focal point intersects the substrate surface to give a continuous line of minimal width. In practice, this represents a formidable engineering task.

Instead, one can conceptualize a narrow aerosol beam that is not focused at some point next to the capillary tip, but collimated such that all the particles have their velocity vectors parallel to the capillary axis. Ideally, one can think of all the particles flying along the capillary axis line. This would be an optimal way of aerosol flow processing which we term here as "collimated aerosol beam", or CAB. In this instance, a deposited line width will not depend critically on the distance between the capillary tip and the substrate. In addition, the line spreading due to particle deflection in the radial shear flow in the vicinity of the substrate is expected to be minimal.

The idea of a focused CAB is not new. Several researchers have successfully focused and collimated aerosol particles using properly designed "aerodynamic lens" systems—series of thin plates with about millimeter size pinholes (Liu et al. 1995a, b; Di Fonzo et al. 2000; Wang et al. 2005a, b, c; Wang and McMurry. 2006). These lens systems were designed for low pressure and particles in the nanometer range, but particles as large as 3 μm have been also used in lens systems. Modeling of the forces on the aerosol particles was accomplished using only the Stokes drag force that accounted for the Cunningham slip correction factor. In particular, it was found that a continuum approximation for the modeling of the Stokes drag force was only applicable for $Kn_p < 0.1$. Wang and McMurry (2006) developed a computer program that determines the correct parameters for an aerodynamic lens system where parameters such as flow rate, pressure, diameter of the lenses, and spacing between lenses were optimized to provide a collimated aerosol stream. The program used values obtained by numerical simulations of the flow of aerosol particles through the lens system.

Here we propose a method of how the focused CAB can be generated through a micro-capillary of slowly varying radius. To prevent the aerosol beam from focusing immediately after exiting the capillary and to collimate the beam, a linearly *converging* micro-capillary (MC1) is connected in series with a linearly *diverging* micro-capillary (MC2) such that radius of the end of MC1 matches with the radius of the beginning of MC2: ($R_2^{(MC1)} = R_1^{(MC2)}$), as shown in Fig. 5a. Collimation of the aerosol is promoted due to the following two reasons: firstly, gas flow diverging in MC2 will drag aerosol particles away from the centerline due to the Stokes drag; and secondly, the gas flow decelerating in MC2 will push the particles to the

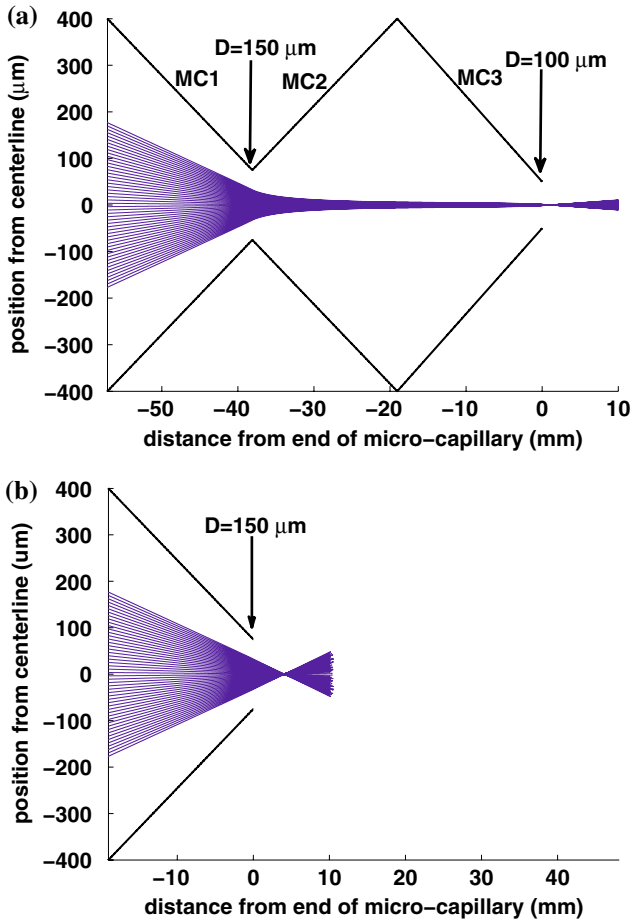

Fig. 5 The theoretically calculated beam width of an aerosol flowing through the CAB system (**a**) and the single MC (**b**). Q = 40 cm^3/min is total gas flowrate; ρ_p = 2000 kg/m^3; a = 0.21 μm particle radius, $\mu = 1.67 \times 10^{-5}$ N s/m^2, and ρ = 1.16 kg/m^3 (nitrogen)

region where the fluid velocity is lower (i.e., away from the center line) due to the Saffman force. If the geometrical parameters of MC1 and MC2 are selected properly, one can expect that the aerosol beam will become almost perfectly collimated inside MC2. However, the velocity of the aerosol beam at the MC2 exit will be so low that the aerosol beam will easily change its direction while approaching the substrate. To prevent the aerosol beam deflection right after the MC2 exit, a third micro-capillary (MC3), linearly *converging*, is connected to the linearly diverging micro-capillary (MC2) such that the radius of the end of MC2 matches with the radius of the beginning of MC3: ($R_2^{(MC2)} = R_1^{(MC3)}$). In the converging MC3, the gas flow will speed up and accelerate the aerosol particles along the capillary centerline.

It is noteworthy that nearly ideal collimation can be theoretically achieved if the converging capillary is matched with a very long micro-capillary of constant diameter of about 100 μm. In this case, aerosol particles dragged by the carrier gas flowing along the capillary would be attracted to the capillary centerline due to the Saffman force. The particles would group at the centerline while flowing through the long capillary, however, clogging would likely result due to the relatively small diameter of the capillary. More research is needed to understand whether such an approach is feasible.

4 The experimental observation of the theoretically predicted focused collimated aerosol beam

Aerosol particles used in the experiments were produced from silver ink from Harima Chemicals Inc. (Product Code NPS-J, Japan) and from Nano-Size LTD (Migdal Ha'Emek, Israel). The Harima ink is a dispersion of 50 nm particles of silver (57–62 wt.%) in *n*-tetradecane solvent (27–34 wt.%) and proprietary dispersant molecules (8–12 wt.%). The overall density of the ink varies from 1,600 to 2,000 kg/m^3. The ink produced by Nano-Size LTD is also a solid-in-liquid dispersion with 30–50% by weight silver nanoparticles ($d \sim 50$ nm) in a solvent mixture (water and ethanol) with up to 3% by weight dispersant.

The nano-ink was atomized via a modified Sonaer Corporation's Sonozap 241PG ultrasonic atomizer operating at 2.4 MHz. A glass ink vial, mounted on translation/rotation stages, was partially submersed in a 25°C temperature controlled water bath (Omega CN9600 series PID and thermoelectric cooler), which is the transmission medium for the ultrasonic energy from the piezo crystal. Dry nitrogen (99.995% purity) flows through the ink vial to produce an aerosol-rich flow.

A sheath flow is inserted annularly around the aerosol flow using an Optomec Inc. M^{3}D system deposition head. The coupled aerosol and sheath flows are directed through a ceramic micro-capillary (single MC) or multiple micro-capillary system (CAB system) where the flow is accelerated and focused. As discussed in Sect. 2, alumina micro-capillaries having a linearly decreasing inner diameter were used. The sheath flow prevents the capillary from clogging by minimizing the initial aerosol beam width and improves the focusing of the aerosol particles. Sheath and aerosol flows are controlled by MKS model M100B01322CP1BV mass flow controllers (up to 200 cm^3/min flow with 1% full-scale accuracy) with a PR4000 MFC interface. Finally, the particles exit the CAB system at a high velocity of the order of 100 m/s allowing deposition onto moving substrates creating lines and patterns. A schematic of the CAB system is shown in Fig. 2.

The aerosol particles focusing in the micro-capillary can be quantified by the width of the aerosol beam without monitoring the trajectories of individual particles. The aerosol beam leaving the CAB system was visualized using

scattered laser light imaged with an Olympus BX60M microscope. The CAB system was rigidly held in place using a 3-axis linear micro-positioner (Newport SDS65 linear stages), mounted to the microscope. The micro-positioner made focusing on the aerosol stream simple and provided distance measurements from the CAB system exit. The total optical magnification of the system ranged from 100× to 1000×, with optical resolution limited by the wavelength of light. A diode pumped solid state (DPSS) 532 nm frequency doubled Nd:YAG laser with a maximum output of 200 mW was directed perpendicularly through the aerosol beam near the micro-capillary end and then into a Kentek ABD-2NP laser beam dump.

The beamwidth was determined at 0.25 mm intervals from the CAB system exit. A total of nine repetitions were carried out on different days to determine the beamwidth deviation due to time variability. Data was taken via a Sony ExWave HAD CCD camera, which records 640 × 480 pixel pictures. The pictures were then transferred to MATLAB where they were normalized and the beamwidth measured using width-at-half-max intensity. The beamwidth at ten different pixel locations around the center of each picture were determined, and the average of these ten was taken as the beamwidth at that respective distance.

We have applied our theoretical model and conducted our experiments for aerosol flow through the CAB system with the following geometrical parameters:

$$\begin{aligned} R_1^{(\mathrm{MC1})} &= 400\ \mu\mathrm{m},\ R_2^{(\mathrm{MC1})} = R_1^{(\mathrm{MC2})} = 75\ \mu\mathrm{m}, \\ R_2^{(\mathrm{MC2})} &= R_1^{(\mathrm{MC3})} = 400\mu m,\ R_2^{(\mathrm{MC3})} = 50\ \mu\mathrm{m}, \\ L^{(\mathrm{MC1})} &= L^{(\mathrm{MC2})} = L^{(\mathrm{MC3})} = 19.05\ \mathrm{mm}. \end{aligned} \tag{15}$$

The theoretically calculated beam width is presented in Fig. 5a. In these calculations the radius of the particles was taken equal to 0.21 μm. This choice was dictated by our preliminary calculations (Akhatov et al. 2007) where the mathematical model was first verified with experiment on aerosol flow in the micro-capillary with a linearly decreasing radius ($R_1 = 400\ \mu$m, $R_2 = 50\ \mu$m, $L = 19.05$ mm). It can also be seen in Fig. 5b that the theoretical model predicts the single MC1 design produces a beam that focuses next to the MC exit and then diverges. The CAB system should be able to focus aerosol beams to a smaller diameter and in certain theoretical cases completely collimate the aerosol particles. According to the simulation (Fig. 5a), the particles are focused to about 5% of the total diameter by the time they reach the third nozzle. It can be seen in Fig. 6 that the experimental beamwidth exiting the CAB system is indeed very narrow.

When compared to the single MC, the beamwidth leaving the CAB nozzle is much thinner and more collimated. Toward that end, the minimum beamwidth is 1.9 μm at 2 mm past the CAB system exit as compared to a minimum

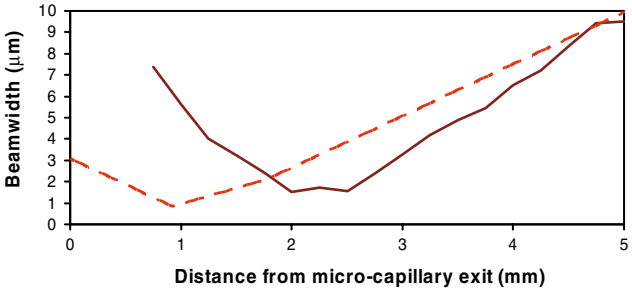

Fig. 6 Aerosol beamwidth vs. distance from the CAB system exit. $Q = 40$ cm^3/min is total gas flowrate; $\rho_p = 2{,}000$ kg/m^3; $\mu = 1.67 \times 10^{-5}$N s/m^2, $\rho = 1.16$ kg/m^3 (nitrogen); *solid line* experimental results, *dashed line* theoretical modeling. Theoretical calculations are for $a = 0.21$ μm particle radius

beamwidth of 5 μm at 1.8 mm past the single MC design exit. The beamwidth remains small even to 5 mm past the CAB system where it has a width of only 12 μm.

It should be noted here that the theoretical model using only the Stokes drag force does not correlate with the experimental data, while the theoretical model that uses both the Saffman and the Stokes drag forces closely matches the experimental data. When comparing the theoretical beamwidth derived from both Stokes and Saffman forces to the experimental data for beamwidth, some variation is noted (Fig. 6). This may be a consequence of non-perfect alignment of the micro-capillaries in the CAB system where the centerlines are not exactly inline and the inner diameters are not symmetric. Improvements in micro-capillary geometry will likely improve the correlation between the theoretical and experimental results.

One important factor for both modeling the aerosol flow and for depositing lines is the size distribution of the aerosol particles. As illustrated in Fig. 7, the size of the

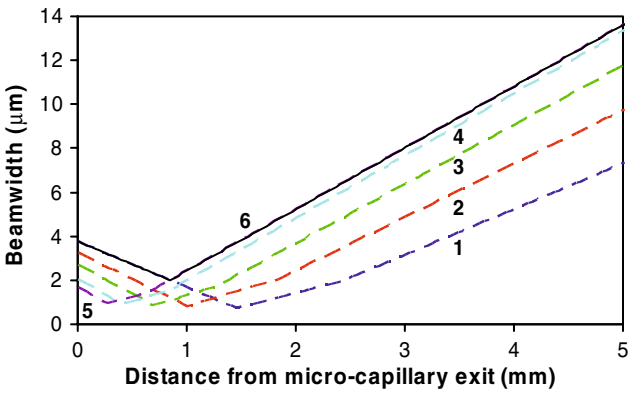

Fig. 7 Theoretical modeling of the aerosol beamwidth versus distance from the CAB system exit for particles of (*1*) 0.3 μm, (*2*) 0.4 μm, (*3*) 0.5 μm, (*4*) 0.6 μm, (*5*) 0.7 μm diameter. *Line* (*6*) represents the superposition of these beamwidths. $Q = 40$ cm^3/min is total gas flowrate; $\rho_p = 2{,}000$ kg/m^3; $a = 0.21$ μm particle radius, $\mu = 1.67 \times 10^{-5}$N s/m^2, and $\rho = 1.16$ kg/m^3 (nitrogen)

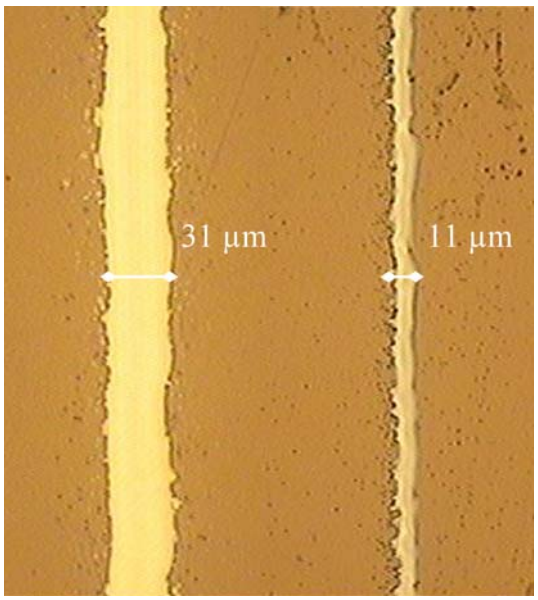

Fig. 8 Unsintered silver lines written with Harima ink. Aerosol flow of 25 cm^3/min, and sheath flow of 15 cm^3/min, stand-off height of 2 mm, translation speed of 30 mm/s, and nitrogen gas. The *left line* is written with the single MC design. The *right line* is written with the CAB system

aerosol particles plays an important role in the beamwidth. If the aerosol flow contained particles of many sizes the overall beamwidth would be increased as seen in line number 6. Further improvement in the morphology of the lines by CAB will require an aerosol flow that is comprised of a mono-disperse population of particles.

An experiment to compare the direct-write performance of the single MC design and the CAB system was devised. Lines were printed on a substrate with Harima ink, an atomizer flow of 25 cm^3/min, a sheath flow of 15 cm^3/min, a stage velocity of 30 mm/s, and a stand-off distance of 2 mm. The linewidths produced by the single MC design and the CAB systems are compared in Fig. 8. The single MC design created lines approximately 31 μm wide and the CAB system produced lines approximately 11 μm wide. Note that the flow parameters were not fully optimized to produce the thinnest lines possible; they were only set to a standard commonly used in the lab. Small process modifications gave a line approximately 9.5 μm wide written with the CAB system (Fig. 9). This line was written on polyimide with silver ink from Nano-Size LTD using the following parameters: 25 cm^3/min aerosol flow, 15 cm^3/min sheath flow, 30 mm/s stage velocity, and a stand-off distance of 2 mm.

Experimental results from the linewidth comparison prove that the beamwidth of the CAB system is thinner than that of the single MC design. The lines written by the CAB system were approximately 1/3 the width of those written by the single MC design under identical processing

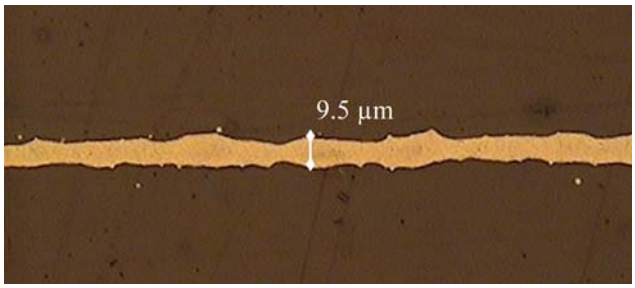

Fig. 9 Unsintered silver line written with Nano-size ink and the CAB system. Aerosol flow of 25 cm^3/min, sheath flow of 15 cm^3/min, translation speed of 30 mm/s, stand-off height of 2 mm, and nitrogen gas

conditions. Additional improvements to the design of the CAB system are anticipated after the effects of aerosol particle size distribution, particle density, and velocity field exiting the micro-capillary are better characterized and understood.

5 Conclusions

This paper is based on the observation that aerosol microflow through a capillary of a diameter ~100 μm and a length ~1 cm, at a relatively high velocity of ~100 m/s, illustrates a new manifestation of the Saffman force in microfluidics where aerosol particles in gas flowing through a micro-capillary are forced to migrate perpendicular to the center line of the capillary (Akhatov et al. 2007). It is shown theoretically and experimentally that it is possible to design a micro-capillary system ("aerosol gun") capable of generating a focused CAB in which aerosol particles stay very close to a capillary centerline. This micro-capillary system consists of a sequence of three slowly converging/diverging/converging micro-capillaries which is termed a CAB system. The performance of such a CAB system for direct-write fabrication on a substrate was demonstrated.

The present CAB-DW system design has not been optimized. The parameters of the slowly converging/diverging micro-capillaries employed in this study were limited to those nozzle geometries that are available commercially. Assuming an adequate mathematical model, future optimization of the CAB-DW system appears to rely on the ability to manufacture slowly converging/diverging micro-capillaries with targeted properties and the existence of a monodisperse aerosol generator. The research presented in this paper is driven by applications of direct-write fabrication technology (Hoey et al. 2007).

Acknowledgments This material is based on research sponsored by the Defense Microelectronics Activity under agreement number H94003-06-2-0601. The United States Government is authorized to

reproduce and distribute reprints for government purposes, notwithstanding any copyright notation thereon. The authors are grateful to Dr. Gregory McCarthy, the director of the NDSU Center for Nanoscale Science and Engineering—for encouraging discussions and for suggesting the term "CAB".

References

Akhatov IS, Hoey JM, Swenson OF, Schulz DL (2007) Aerosol focusing in micro-capillaries: theory and experiment. J Aerosol Sci (submitted)

Batchelor GK (2000) An introduction to fluid dynamics. Cambridge University Press, Cambridge

Bracht K, Merzkirch W (1979) Dust entrainment in a shock-induced, turbulent air flow. Int J Multiphase Flow 15(5):301

Carlson DJ, Hoglund RF (1964) Particle drag and heat transfer in rocket nozzles. AIAA J 2(11):1980

Cunningham E (1910) On the velocity of steady fall of spherical particles through fluid medium. Proc Soc Lond Ser A 83:357–365

Dahneke B, Friedlander SK (1970) Velocity characteristics of beams of spherical polystyrene particles. J Aerosol Sci 1:325–339

Dandy DS, Dwyer HA (1990) A sphere in a shear flow at finite Reynolds number: effect of shear on particle lift, drag, and heat transfer. J Fluid Mech 216:381–410

Di Fonzo F, Gidwani A, Fan MH, Neumann D, Iordanoglu DI, Heberlein JVR, McMurry PH, Girshick SL, Tymiak N, Gerberich WW, Rao NP (2000) Focused nanoparticles-beam deposition of patterned microstructures. Appl Phys Lett 77(6):910–912

Fernandez de la Mora J, Riesco-Chueca P (1988) Aerodynamic focusing of particles in a carrier gas. J Fluid Mech 195:1–21

Fletcher B (1976) The interaction of a shock with a dust deposit. J Phys D Appl Phys 9(2):197–202

Fuerstenau S, Gomez A, Fernandez de la Mora J (1994) Visualization of aerodynamically focused subsonic aerosol jets. J Aerosol Sci 25:165–173

Gerrard JH (1963) An experimental investigation of the initial stages of the dispersion of dust by shock waves. Br J Appl Phys 14:186–192

Hishida M, Hayashi AK (1989) Numerical simulation of a shock wave–solid particle interaction. In: Proceedings of international symposium on computational fluid dynamics, Nagoya, Japan, pp 1055–1060

Hoey JM, Akhatov IS, Swenson OF, Schulz DL (2007) Focusing of aerosol particles. US Provisional Patent Application # 60/956,493

Hwang CC (1986) Initial stages of the interaction of a shock wave with a dust deposit. Int J Multiphase Flow 12(4):655–666

Israel GW, Friedlander SK (1967) High-speed beams of small particles. J Colloid Interface Sci 24:330–337

Israel GW, Wang JS (1971) Dynamical properties of aerosol beams. Technical note BN-709. Institute for Fluid Dynamics and Applied Mathematics, University of Maryland

Karniadakis G, Beskok A, Aluru N (2005) Microflows and Nanoflows: fundamentals and simulation. Springer, Berlin

Knudsen M, Weber S (1911) Luftwiderstand gegen die langsame Bewegung kleiner Kugeln. Amm Physics 36:981–994

Lauga E, Brenner MP, Stone HA (2005) Microfluidics: the no-slip boundary condition. In: Foss J, Tropea C, Yarin A (eds) Springer handbook of experimental fluid dynamics. Springer, Berlin

Li Z, Wang H (2003) Drag force diffusion coefficient, and electric mobility of small particles. I. Theory applicable to the free-molecule regime. Phys Rev 68:061206

Lipatov GN, Grinshpun SA, Semenyuk TI (1989) Properties of crosswise migration of particles in ducts and inner aerosol deposition. J Aerosol Sci 20(8):935–938

Liu P, Ziemann PJ, Kittelson DB, McMurry PH (1995a) Generating particle beams of controlled dimensions and divergence: I. Theory of particle motion in aerodynamic lenses and nozzle expansions Aerosol Sci Technol 22(3):293–313

Liu P, Ziemann PJ, Kittelson DB, McMurry PH (1995b) Generating particle beams of controlled dimensions and divergence: II. Experimental evaluation of particle motion in aerodynamic lenses and nozzle expansions. Aerosol Sci Technol 22(3):314–324

Mei R (1992) An approximate expression for the shear lift force on a spherical particle at finite Reynolds number. Int J Multiphase Flow 18(1):145–147

Merzkirch W, Bracht K (1978) The erosion of dust by a shock wave in air: initial stages with laminar flow. Int J Multiphase Flow 4(1):89–95

Millikan RA (1923) Coefficients of slip in gases and the law of reflection of molecules from the surface of solids and liquids. Phys Rev 21(3):217–238

Osiptsov AN (1988) Motion of dusty gas at the entrance to a flat channel and a circular pipe. Fluid Dyn 23(6):867–874

Osiptsov AN (1997) Mathematical modeling of dusty-gas boundary layers. Appl Mech Rev 50(6):357–370

Pique A, Chrisey DB (eds) (2002) Direct write technologies for rapid prototyping applications. Academic, San Diego

Rao NP, Navascues J, Fernandez de la Mora J (1993) Aerodynamic focusing of particles in viscous jets. J Aerosol Sci 24(7):879–892

Renn MJ, Marquez G, King BH, Essien M, Miller WD (2002) Flow- and laser-guided direct write of electronic and biological components. Direct write technologies for rapid prototyping applications. In: Pique A, Chrisey DB (eds) Academic, San Diego, pp 475–492

Saffman PG (1965) The lift on a small sphere in a slow shear flow. J Fluid Mech 22:385–400

Saffman PG (1968) Corrigendum. J Fluid Mech 31:624

Wang B, Xiong Y, Osiptov AN (2005a) Two-way coupling model for shock-induced laminar boundary-layer flows of a dusty gas. Acta Mech Sin 21:557–563

Wang X, Gidvani A, Girshick SL, McMurry PH (2005b) Aerodynamic focusing of nanoparticles: II. Numerical simulation of particle motion through aerodynamic lenses. Aerosol Sci Technol 39:624–636

Wang X, Kruis FE, McMurry PH (2005c) Aerodynamic focusing of nanoparticles: I. Guidelines for designing aerodynamic lenses for nanoparticles. Aerosol Sci Technol 39:611–623

Wang X, McMurry PH (2006) A design tool for aerodynamic lens systems. Aerosol Sci Technol 40:320–334